Polish Society of Composite Materials
Polskie Towarzystwo Materiałów Kompozytowych

16: 2 (2016) 74-78

COMPOSITES THEORY AND PRACTICE

Dariusz Garbiec

Metal Forming Institute, ul. Jana Pawła II 14, 61-139 Poznan, Poland
Corresponding author. E-mail: dariusz.garbiec@inop.poznan.pl

Received (Otrzymano) 26.01.2016

CONSOLIDATION OF Mg-SiC COMPOSITES BY SPARK PLASMA SINTERING

Mg based MMCs are increasingly used in automotive and aerospace applications. In this paper, Mg-SiC composites were obtained by the spark plasma sintering method. Various volume contents of SiC particles (5, 10, 15, 20 and 30 vol.%) were used. The samples have near full density, over 98%, and SEM observations confirmed the near full density of the sintered compacts. However, there was an optimum SiC content above which agglomeration of the SiC particles in the microstructure of the composites occurred. Moreover XRD analyses showed that besides Mg and α-SiC, β-SiO_2 (low-temperature β-quartz) and Mg_2Si phases are also present. The mechanical tests results demonstrate that the hardness and compressive strength of the obtained composites tend to increase with an increasing SiC volume content at the expense of compressive strain. The best results of hardness (111 $HV_{0,5}$) and compressive strength (346 MPa) were obtained by the Mg-30%SiC composite.

Keywords: Mg-SiC composite, spark plasma sintering, powder metallurgy, mechanical properties

KONSOLIDACJA KOMPOZYTÓW Mg-SiC METODĄ ISKROWEGO SPIEKANIA PLAZMOWEGO

Metalowe materiały kompozytowe na bazie Mg są coraz częściej wykorzystywane w przemyśle motoryzacyjnym i lotniczym. W niniejszej pracy do wytworzenia kompozytów Mg-SiC wykorzystano metodę iskrowego spiekania plazmowego. Zastosowano różne udziały objętościowe cząstek SiC (5, 10, 15, 20 i 30% obj.). Uzyskane spieki odznaczają się gęstością względną zbliżoną do gęstości materiału litego wynoszącą powyżej 98%, co potwierdziły obserwacje za pomocą SEM. Ponadto analiza XRD wykazała w strukturze poza Mg i α-SiC obecność faz β-SiO_2 (kwarc niskotemperaturowy β) i Mg_2Si. Wyniki badań właściwości mechanicznych wskazują, że twardość i wytrzymałość na ściskanie zwiększa się wraz ze wzrostem udziału objętościowego SiC przy jednoczesnym zmniejszeniu odkształcenia. Największą twardością (111 $HV_{0,5}$) oraz wytrzymałością na ściskanie (346 MPa) odznacza się kompozyt Mg-30%SiC.

Słowa kluczowe: kompozyt Mg-SiC, iskrowe spiekanie plazmowe, metalurgia proszków, właściwości mechaniczne

INTRODUCTION

Magnesium (Mg) and its alloys are increasingly popular metals in automotive and aerospace applications. It results mainly from the low density (1.74 g/cm^3) of Mg, which facilitates reducing fuel consumption and greenhouse gas emissions [1, 2]. Beside this, Mg and its alloys also possess several other benefits such as high specific strength [2, 3], good machinability [1, 4], dimensional stability [2, 4], high damping capacity [1, 3, 4], electromagnetic radiation resistance [4] and low power consumption [1, 4]. Serious disadvantages of Mg and its alloys are their low ductility and rapid loss of strength at elevated temperatures, which limits their use in demanding structural applications [1]. One of the steps in order to improve some of the mechanical properties of Mg and its alloys is to produce metal matrix composites (MMCs) based on Mg and its alloys [5-7]. Engineering parts made from Mg-based MMCs are fabricated by stir casting [7], disintegrated metal deposition [8], melt infiltration [9], powder metallurgy (PM) etc. Many research programs have shown that PM is an important and useful processing route for the fabrication of MMCs and a number of studies have used PM techniques for fabricating Mg based MMCs [10, 11]. A promising one is spark plasma sintering (SPS). Using SPS Muhammad et al. [1] obtained Mg-SiC (5, 10 and 15 wt.%) composites. They proved that sintering Mg below 525°C is not effective in view of the occurrence of significant porosity. They suggest that the temperature of spark plasma sintering of Mg should range from 525 to 585°C, so that the maximum sintering temperature is lower than the melting point of magnesium (657°C). However, in view of the SPS process character, the local temperature in the contact area of the Mg particles would be higher as compared to other PM techniques.

In this study, the authors used SPS to fabricate Mg-SiC (5÷30 vol.%) composites. The goal of the investigations was to fabricate near full dense Mg based MMCs in a short time and determine the effect of various volume contents of SiC reinforcement on the

microstructure and some mechanical properties of the obtained composites, which might be used as a material for applications in automotive and aerospace. The process parameters were determined in preliminary studies of spark plasma sintering Mg powder, and the sintering temperature of 550°C, holding time 5 min, heating rate 100°C/min and compaction pressure of 50 MPa are the optimal SPS regimes. Matin et al. [7] used similar SPS regimes to obtain Mg-TiNi (10÷30 vol.%) composites and Aldica et al. [12] showed that the heating rate of ~ 100°C/min is optimum for the SPS process of MgB_2.

MATERIALS AND METHODS

Mg (99.8% purity) and SiC (99.0% purity) starting powders supplied from Kamb Import-Export, Poland were mechanically mixed using a mixer, similar to a Turbula shaker-mixer. The obtained Mg/SiC (5, 10, 15, 20, 30 vol.%) powder mixtures were then densified by spark plasma sintering using an HP D 25-3 furnace (FCT, Germany). The powder mixtures were heated up to 550°C at 100°C/min in vacuum of 5 Pa and held at the sintering temperature for 5 min. The pressure level on the specimens was kept constant at 50 MPa throughout the sintering process. The temperature was monitored by an optical pyrometer through a non-through hole in the graphite upper punch. From the spark plasma sintered compacts with dimensions of ø40x10 mm, samples for tests were cut by the wire electrical discharge machining.

Particle size distribution using the laser diffraction technique was carried out by a Mastersizer 3000 (Malvern, UK) analyzer. The density of the specimens was measured by the Archimedes method. X-ray structural studies were performed using a Kristalloflex 4 (Siemens, Germany) diffractometer. The tests were performed using MoK_α radiation with 2Θ 15÷55°. The microstructures of the sintered compacts were observed on polished and etched by nital cross-sectioned surfaces by SEM using an Inspect S (FEI, Netherlands) microscope. Vickers hardness measurements using a hardness tester FV-800 (Future-Tech, Germany) were carried out by applying a load of 4.903 N for 15 s. The compressive strength was measured without lubricant using a 4483 Instron mechanical testing machine of the measuring range of up to 150 kN (constant crosshead speed) with the initial strain rate of 0.0033 s^{-1}. For the tests, samples with dimensions of ø10x10 mm were used.

RESULTS AND DISCUSSION

Figure 1 shows the morphology and particle size distribution of the Mg and SiC powders. The particles of the Mg powder are generally rounded in shape and elongated in contrast to the particles of the SiC powder which are angular in shape. The median particle size of Mg is 35.90 µm and SiC is 4.04 µm. The other particle size distribution parameters are presents in Table 1.

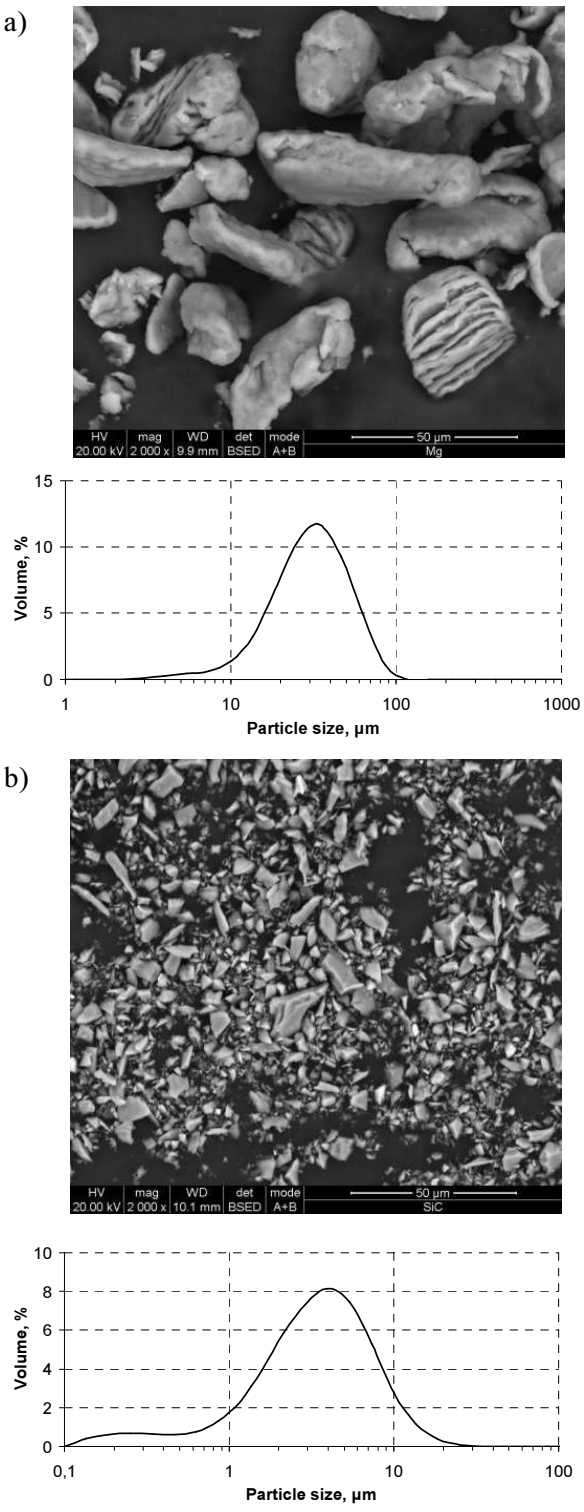

Fig. 1. Morphology of powder particles and particle size distribution of: a) Mg and b) SiC

Rys. 1. Morfologia cząstek proszku oraz rozkład wielkości cząstek dla: a) Mg oraz b) SiC

TABLE 1. **Particle size distribution D_{10}, D_{50} and D_{90} of Mg and SiC powder**

TABELA 1. **Rozkład wielkości cząstek D_{10}, D_{50} i D_{90} proszku Mg oraz SiC**

Powder	D_{10} [µm]	D_{50} [µm]	D_{90} [µm]
Mg	17.20	35.90	65.70
SiC	1.14	4.04	9.60

For a better understanding of the spark plasma sintering of the Mg/SiC powder mixtures, X-ray diffraction analyses were carried out. In the Mg-SiC system, there are not many possible phases that can be formed [13]. The phases presented in the spark plasma sintered compacts are shown in Figure 2.

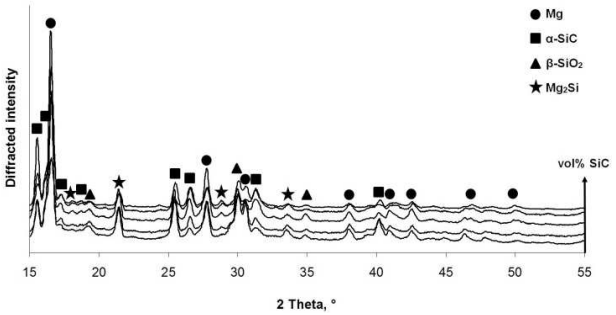

Fig. 2. X-ray diffraction spectra of spark plasma sintered Mg-SiC composites

Rys. 2. Dyfraktogramy kompozytów Mg-SiC wytworzonych metodą SPS

In the sintered compacts, besides Mg and α-SiC, β-SiO_2 (low-temperature β-quartz) and Mg_2Si phases are also present. Braszczynska et al. [14] explained that SiC tend to be covered with SiO_2 film, due to the natural oxidation effect, even at ambient temperature. Normally, oxide films are evaporated during the SPS process but in some cases, the oxide films may still exist along the particle boundaries, especially in the cases of SiC particles which are not electrically conductive, and during the SPS process the generation of spark discharges between the particles is inhibited, therefore a high temperature on the particle surfaces is not generated and finally the evaporation of oxide films is limited [1, 15]. The presence of Mg_2Si phase in the structure of Mg-SiC composites was explained by Malik et al. [16]. In the SPS process it results from the contact of SiC particles covered by SiO_2 film with the molten surface of the Mg particles, which leads to formation of the Mg_2Si phase due to the reaction of Mg and SiO_2.

The spark plasma sintered microstructures were observed on cross-sections made perpendicular to the pressing direction. As shown in the SEM micrographs in Figure 3, Mg and SiC particles and a small amount of residual porosity, especially in the sintered compacts with a high volume content of SiC particles, are visible. The SiC particles are almost uniformly distributed along the Mg boundary in the composites with a volume content of SiC particles up to 10 vol.%. With an increasing volume content of SiC particles, agglomerations of SiC particles were detected. The same relationship was observed by Muhammad et al. [1]. They conclude that this phenomenon results from an inadequate ratio of surface area between the Mg and SiC particles. Slipenyuk at al. [17] proved that there is a theoretical limit for the particle reinforcement concentration in the PM processed composites, at which the reinforcement particles can still be uniformly distributed in the material. This limit depends on the matrix-to-reinforcement particle size ratio, the matrix and reinforcement particle shape and the processing method.

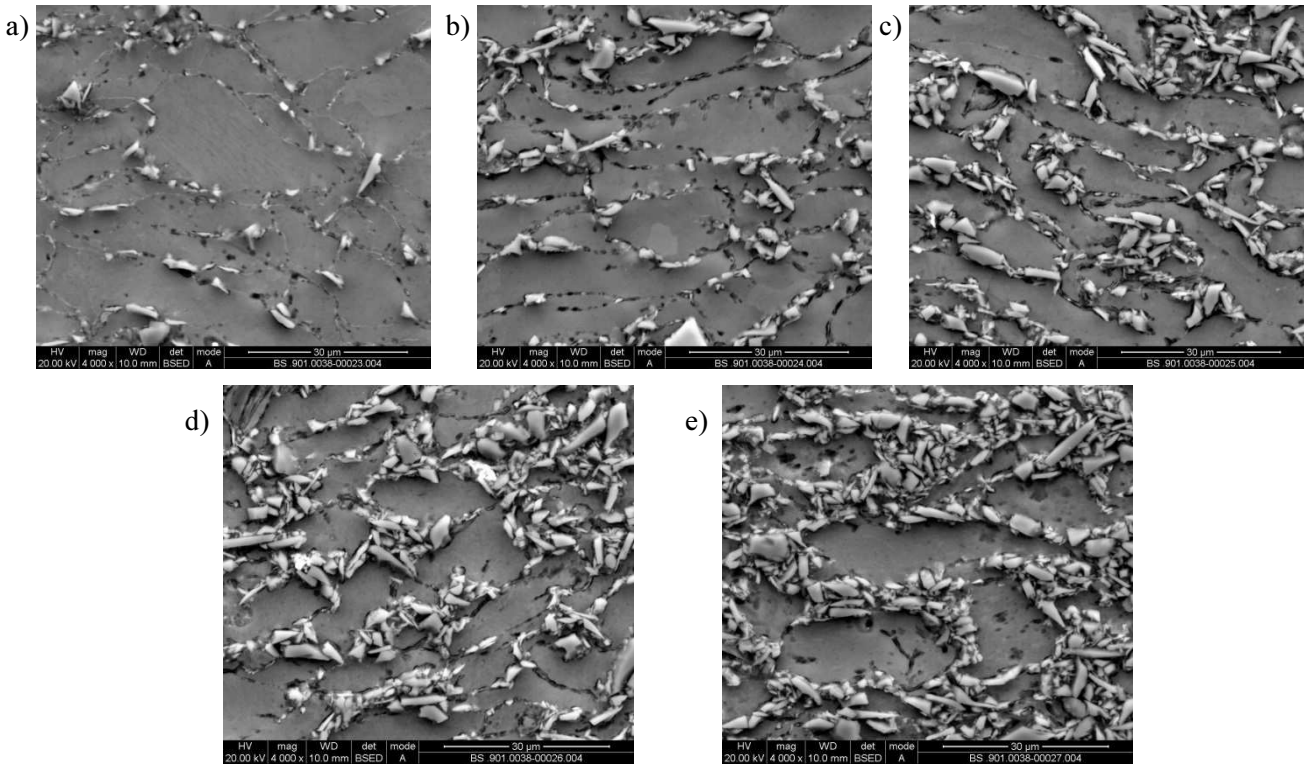

Fig. 3. Microstructure of spark plasma sintered Mg-SiC composite: a) 5 vol.% SiC, b) 10 vol.% SiC, c) 15 vol.% SiC, d) 20 vol.% SiC, e) 30 vol.% SiC

Rys. 3. Mikrostruktura kompozytów Mg-SiC wytworzonych metodą SPS: a) 5% obj. SiC, b) 10% obj. SiC, c) 15% obj. SiC, d) 20% obj. SiC, e) 30% obj. SiC

Table 2 shows the influence of various volume contents of SiC particles on the relative density, hardness and compressive strength of the spark plasma sintered Mg-SiC composites. The density measurements results reveal that an increasing content of SiC particles in the composites has an influence on the relative density of the obtained sintered compacts. Almost full density was attained with a content of SiC particles up to 15% and near full density over 98% was attained at each content of SiC particles. From these results, it can be concluded that SPS is an effective technique for the consolidation of Mg-SiC composites.

TABLE 2. **Relative density, hardness and compressive strength of spark plasma sintered Mg-SiC composites (± - standard deviation)**

TABELA 2. **Gęstość względna, twardość oraz wytrzymałość na ściskanie kompozytów Mg-SiC wytworzonych metodą SPS (± - odchylenie standardowe)**

Vol.% SiC	Relative density [%]	Hardness [$HV_{0.5}$]	Compressive strength [MPa]
0	99.83 ±0.07	53 ±2	221 ±1
5	99.79 ±0.06	65 ±3	243 ±4
10	99.71 ±0.05	74 ±4	272 ±4
15	99.59 ±0.10	86 ±3	281 ±7
20	99.31 ±0.11	109 ±4	301 ±7
30	98.03 ±0.15	111 ±4	346 ±17

The relationship between Vickers hardness and the volume content of SiC particles in the obtained composites shows that hardness increases with an increasing content of SiC particles from 53 $HV_{0.5}$ for Mg to 111 $HV_{0.5}$ for the Mg-30%SiC composite. Muhammad et al. [1] also showed the increase in hardness with an increasing SiC content for Mg-SiC composites synthesized by SPS technology. The hardness obtained by their experiments was about 73 $HV_{0.05}$. This value is lower than the hardness of 86 $HV_{0.5}$ obtained in the present study, which is probably due to the higher content of SiC particles in this study in view of the volume content opposed to weight content in their work, or by applying a four-times higher heating rate. A high heating rate is advantageous because it reduces sintering time and promotes densification without significant grain growth, but it should be kept in mind that the impact of heating rates is dependent on the material and particle size [12]. For example, a high heating rate is desirable for the spark plasma sintering of WC-Co composites [18], but low for WB ceramics [19]. The compressive strength for the spark plasma sintered Mg-SiC composites also increases with an increasing content of SiC particles from 221 MPa for Mg to 346 MPa for the Mg-30%SiC composite, but the compressive strain (ductility) decreased, which is clearly show in the compressive stress-strain curves presented in Figure 4.

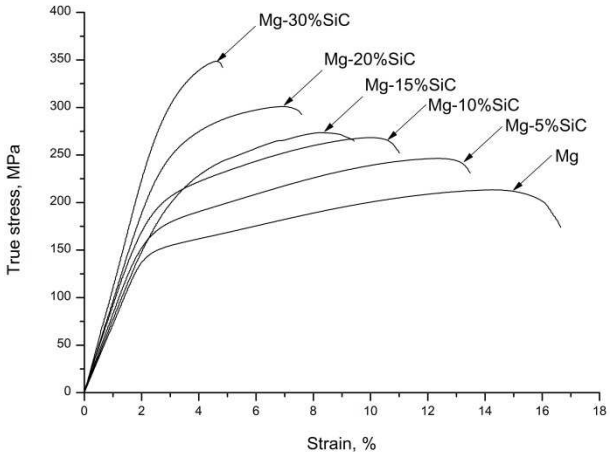

Fig. 4. Stress-strain curves of spark plasma sintered Mg-SiC composites

Rys. 4. Krzywe naprężenie-odkształcenie kompozytów Mg-SiC wytworzonych metodą SPS

CONCLUSIONS

In this paper the consolidation of Mg/SiC powder mixtures with various volume contents of SiC particles using SPS technology was investigated. All the presented results revealed that SPS is an effective technique to obtain Mg-SiC composites characterized by near full density (over 98%) and hardness up to 111 $HV_{0.5}$ and compressive strength up to 346 MPa. X-ray diffraction analyses showed that in all cases, besides Mg and α-SiC, low-temperature β-quartz and Mg_2Si phases are also present. Moreover, the SEM observations showed that in the composites with a volume content of SiC particles over 10 vol.%, agglomerations of SiC particles are present.

Acknowledgement

The study was realized within the framework of statutory work BS 901 38 of the Metal Forming Institute in Poznan, entitled "Manufacturing innovative materials for application in modern branches of economy by the techniques of powder metallurgy".

REFERENCES

[1] Muhammad W.N.Z.W., Sajuri Z., Mutoh Y., Miyashita Y., Microstructure and mechanical properties of magnesium composites prepared by spark plasma sintering technology, J. Alloys Compd. 2011, 509, 6021-6029.

[2] Falcon-Franco L., Garcia-Villarreal S., Curiel F.F., Arizmendi-Morquecho A., Synthesis of magnesium metallic matrix composites and the evaluation of aluminum nitride addition effect, J. Alloys Compd. 2016, 663, 407-412.

[3] Aydogmus T., Processing of interpenetrating Mg-TiNi composites by spark plasma sintering, Mater. Sci. Eng. A 2015, 624, 261-270.

[4] Fida Hassan S., Nasirudeen O.O., Al-Aqeeli N., Saheb N., Patel F., Baig M.M.A., Magnesium-nickel composite:

Preparation, microstructure and mechanical properties, J. Alloys Compd. 2015, 646, 333-338.

[5] Huang S.-J., Ho Ch.-H., Feldman Y., Tenne R., Advanced AZ31 Mg alloy composites reinforced by WS_2 nanotubes, J. Alloys Compd. 2016, 654, 15-22.

[6] Labib F., Mahmudi R., Ghassemi H.M., Impression creep behavior of extruded Mg-SiC_p composites, Mater. Sci. Eng. A 2015, 640, 91-97.

[7] Matin A., Fereshteh Saniee F., Reza Abedi H., Microstructure and mechanical properties of Mg/SiC and AZ80/SiC nan-composites fabricated through stir casting method, Mater. Sci. Eng. A 2015, 625, 81-88.

[8] Gupta M., Lai M.O., Saravanaranganathan D., Synthesis, microstructure and properties characterization of disintegrated deposited Mg/SiC composites, J. Mater. Sci. 2000, 35, 2155-2165.

[9] Contreras A., López V.H., Bedolla E., Mg/TiC composites manufactured by pressureless melt infiltration, Scr. Mater. 2004, 51, 249-253.

[10] Bettles C.J., Magnesium Powder Metallurgy: Process and Materials Opportunities, J. Mater. Eng. Perform. 2008, 17, 297-301.

[11] Burke P., Kipouros G.J., Development of Magnesium Powder Metallurgy AZ31 Alloy Using Comercially Available Powders, High Temp. Mater. Processes (London) 2011, 30, 51-61.

[12] Aldica G., Burdusel M., Popa S., Enculescu M., Pasuk I., Badica P., The influence of heating rate on superconducting characteristics of MgB_2 obtained by spark plasma sintering, Physica C 2015, 519, 184-189.

[13] Stelnacher M., Mrvar P., Zupanlc F., Interfaces in the magnesium-matrix composites, RMZ M&G 2013, 60, 239-247.

[14] Braszczynska K.N., Litynska L., Zyska A., Baliga W., TEM analysis of the interfaces between the components in magnesium matrix reinforced with SiC particles, Mater. Chem. Phys. 2003, 81, 326-328.

[15] Zhang L. M., Gu X. F., Zhang D. M., Yang M. J., SiCp/Al composites fabricated by spark plasma sintering, Ceram. Trans. 2006, 194, 133-141.

[16] Malik M.A., Braszczynska-Malik K.N., Majchrzak K., Microstructural characterization of cast magnesium matrix composites by raman microscopy, Archives of Foundry Engineering 2013, 13, 95-98.

[17] Slipenyuk A., Kuprin V., Milman Y., Goncharuk V., Eckert J., Properties of P/M processed particle reinforcement metal matrix composites specified by reinforcement concentration and matrix-to-reinforcement particle size ratio, Acta Mater. 2006, 54, 157-166.

[18] Garbiec D., Siwak P., Jakubowicz J., The effect of heating rate and sintering time on properties of WC-6Co nanocrystalline composites produced by spark plasma sintering, Composites Theory and Practice 2015, 15, 48-53.

[19] Moscicki T., Radziejewska J., Hoffman J., Chrzanowska J., Levintant-Zayonts N., Garbiec D., Szymanski Z., WB_2 to WB_3 phase change during reactive spark plasma sintering and pulsed laser ablation/deposition processes, Ceram. Int. 2015, 41, 8273-8281.

